Title: A Subtype of Adult-Born Neuron in Male Zebra Finch HVC Expresses DARPP-32 and Does Not Project to RA as part of the Vocal Motor Pathway

Abbreviated Title: Subtypes of Adult-Born Neurons in Zebra Finch HVC

[1]Jake V Aronowitz, [2]Hyekyung Moon, [1,2]John R Kirn, [3]Carolyn L Pytte, & [1,2]Gloster B Aaron

[1]Department of Biology, Wesleyan University, Middletown, CT, USA

[2]Department of Neuroscience and Behavior, Wesleyan University, Middletown, CT, USA

[3]Department of Psychology, Queens College and The Graduate Center, City University of New York, Flushing, NY, USA

Corresponding Author: Jake V. Aronowitz, MA, Jaronowitz@wesleyan.edu, Department of Biology, Wesleyan University, 45 Wyllys Avenue, Middletown, CT, 06457, 860-685-3785

Hyekyung Moon, MA – Boston Children's Hospital, Department of Anesthesiology, Critical Care and Pain Medicine, Randolph Research Lab, Enders Building, 61 Binney St, Boston, MA, 02115, Hyekyungmoon@gmail.com, 617-919-4640;

John R. Kirn, PhD – Department of Biology, Department of Neuroscience & Behavior, Wesleyan University, 45 Wyllys Ave, Middletown, CT, 06457, Jrkirn@wesleyan.edu

Carolyn L. Pytte, PhD – Department of Psychology, Queens College and The Graduate Center, City University of New York, Flushing, NY, 11367, Carolyn.Pytte@qc.cuny.edu, 718-997-4528.

Gloster B. Aaron, PhD – Department of Biology, Department of Neuroscience & Behavior, Wesleyan University, 45 Wyllys Ave, Middletown, CT, 06457, 860-685-3197, Gaaron@wesleyan.edu. Contributions: designed research, wrote the paper.

Acknowledgements: The authors would like to thank Dr. Luke Remage-Healey for helpful comments on earlier versions of the manuscript.

Dedications: This work is dedicated to Dr. John R Kirn who died on November 10th, 2019. His intellect, kindness and patience will be remembered by all those who were lucky enough to know him.

Number of pages: 26

Number of Figures: 8

Number of words – Abstract: 179

Number of words – Introduction: 491

Number of words – Discussion: 1321

Conflict of interest statement: The authors declare no competing financial interests.

Abstract: Adult male zebra finches (*Taeniopygia guttata*) continually incorporate adult-born neurons into HVC, a telencephalic brain region necessary for the production of learned song. These neurons express immediate early genes following song production, suggesting a role for neurogenesis in song production throughout the lifespan. Half of these adult-born HVC neurons (HVC NNs) send their axons to RA as part of the vocal motor pathway underlying learned song production, but the other half do not, and their identity remains unknown. Here we used cell birth-dating, retrograde tract tracing, and immunofluorescence to demonstrate that half of all HVC NNs express the neuron-specific phosphoprotein DARPP-32, a protein associated with DA receptor expression. We also demonstrate that DARPP-32+ HVC NNs are contacted by tyrosine hydroxylase immunoreactive fibers suggesting that they receive catecholaminergic input, are transiently larger than DARPP-32-negative HVC NNs, and do not send axons to RA as part of the vocal motor pathway. Taken together, these findings indicate the existence of a class of HVC NNs that do not project to RA and may constitute the aforementioned unknown half of all HVC NNs.

Introduction

Songbirds, including zebra finches (*Taeniopygia guttata*), continually incorporate new neurons into brain regions that subserve song learning, perception, and production (Kirn & Devoogd, 1989; Sohrabji, et al., 1993; Pytte, 2016). The premotor brain region, HVC (proper name), which is necessary for learned song production, incorporates new neurons throughout adulthood, and these neurons express immediate early genes following song production (Jarvis, et al., 1998; Tokarev, et al., 2016). Approximately half of all new neurons that are added to HVC (HVC NNs) in adult male zebra finches send their axons to the robust nucleus of the arcopallium (RA), a premotor relay and the first synaptic target of the vocal motor pathway underlying song production (Figure 1; Kirn, et al., 1991, 1999). In male zebra finches, 42% of HVC NNs project to RA (HVC_{RA}) at 30 days post-mitosis, and this increases to only 50% at survival times from 3 months to 4 years after cell birth-dating (Scotto-Lomassese, et al., 2007; Walton, et al., 2012). Interestingly, the other half of these new neurons are unaccounted for by known HVC population types. HVC NNs do not project to the basal ganglia homologue Area X, one of the three known projection targets of HVC (Kirn, et al., 1991, 1999; Scharff, et al., 2000). Other researchers have considered two broad explanations for the identity of non-RA projecting HVC NNs: 1) they are HVC_{RA} neurons that do not transport retrograde tracers to their soma for unknown reasons, or 2) they are not HVC_{RA} neurons, but rather project locally within HVC, or to some other brain region (e.g. Nucleus Avalanche, Av). Inhibitory interneurons (HVC_{INT}) may be generated in HVC of juvenile male zebra finches (Scott & Lois, 2007), but this has not been replicated in adults (Scotto-Lomassese, et al., 2007; Walton, et al., 2012). This suggests that non-RA-projecting HVC NNs are 1) excitatory interneurons, 2) local inhibitory interneurons that do not express any of the markers of inhibitory interneurons used in other studies (Wild, et al., 2005;

Scotto-Lomassese, et al., 2007; Walton, et al., 2012), 3) Av-projecting neurons (HVC_{AV}), or 4) HVC_{RA} neurons that fail to transport the retrograde tracer, perhaps due to their axon or synapse type. To our knowledge, there have been no studies revealing the identifying features of these non-RA-projecting HVC NNs.

Here, we used cell birth-dating, immunohistochemistry, and retrograde tracing to characterize the non-RA-projecting HVC NNs. First, we show that nearly half of HVC NNs express DARPP-32 ("DARPP-32+ HVC NNs"). DARPP-32 (DA and cAMP regulated phosphoprotein, 32 kDa) is a neuron-specific phosphoprotein located in the cytoplasm, axons, axon terminals, and dendrites of dopaminoceptive neurons (Walaas & Greengard, 1984; Ouimet & Greengard, 1990). We also demonstrate that DARPP-32+ HVC NNs do not project to RA, have transiently larger nuclei than DARPP-32-neg HVC NNs, and are contacted by tyrosine hydroxylase (TH) fibers. We propose that DARPP-32+ HVC NNs comprise a unique subpopulation of HVC NNs and represent the uncharacterized 50% of HVC NNs in adult-male zebra finches.

Materials and Methods

Animals

All procedures were performed in accordance with the Wesleyan University Institutional Animal Care and Use Committee (IACUC) regulations. Adult male zebra finches (0.5 to 7 years old) were hatched in the Wesleyan University breeding colony. Females were not included in this study because the zebra finch song system is sexually dimorphic, and female HVC is small and does not receive many new neurons in juveniles or adulthood (Burek, et al., 1994; DeWulf & Bottjer, 2005; Shaughnessy, et al., 2019). Birds in this study came from individual family breeding cages with one nest, or from larger cages with two nests. Birds reared in either these

conditions were balanced across groups to control for any effect of juvenile housing condition. When birds reached 90 days post hatch (dph), they were moved from the breeding colony into larger cages where they were group-housed with similarly aged males. Songbirds housed with other males show greater proliferative activity (Shevchouk, et al., 2017), and so we housed our experimental birds in auditory and visual contact of other males to maximize new neuron production. Zebra finches used for time course dependent DARPP-32 expression experiments (n=37, 100-301 dph) were randomly distributed into 7 groups that differed in the amount of time between final BrdU injection and the date of sacrifice. Tissue from birds in this first cohort was also used for tyrosine hydroxylase experiments (n=3, age range: 169-203 dph) and nuclear diameter experiments (n=10, age range: 164-301 dph). We also examined DARPP-32+ neurons in HVC as a function of bird age in a separate set birds (n=17, age range: 1.98 to 6.99 years old). We supplemented this cohort by including tissue from younger animals (n=6, age range: 197-321 dph) randomly selected from our first cohort of young birds. For retrograde tracing experiments, we used a separate group of adult male zebra finches (n=4, age range: 144-175 dph).

BrdU Injections

Zebra finches received 50 µl intramuscular (I.M.) injections of 2-Bromo-5'-deoxyuridine (BrdU; Roche Diagnostics) in 0.05 M Tris buffered saline (TBS; pH=7.4; 15 mg/ml) into the pectoralis muscle twice daily for three consecutive days to label dividing cells. BrdU is bioavailable for approximately 1-2 hours following I.M. injection (Barker, et al., 2013), so injections were performed at least two hours apart. We performed the first injection ~ 10 AM and the second injection ~ 5 PM to avoid differences in circadian rhythms that could affect the amount of new neuron labeling.

Stereotaxic Surgery

28 days following the last BrdU injection, birds (n=4, Fig. 5) were anesthetized with I.M. injections of ketamine and xylazine (0.03 ml of 10 mg/ml ketamine; 0.03 ml of 20 mg/ml xylazine) and placed in a customized stereotaxic apparatus with their head at a 45º angle to the horizontal plane. A midline incision was made on the dorsal surface of the head to expose the skull. A small craniotomy (~0.5 mm^2) was then made above the bifurcation of the midsagittal sinus (Y-point) and the stereotaxis was 'zeroed' at this Y-point (Nixdorf-Bergweiler & Bischof, 2007). Small craniotomies (~1 mm^2) were made over the injection sites for RA: A/P = -1.7 mm, -1.9 mm; M/L= ± 2.65 mm; D/V= -2.3 mm, -2.5 mm. Injections were made at a 9º angle off the vertical axis to avoid damage to HVC en route to RA. The pia was then gently punctured with a 26.5-gauge beveled syringe needle. A 2% Fluorogold solution in 0.9% NaCl ("FG"; Fluorochrome, Inc.) was slowly pressure injected, ~100 nl per site. Following injections, the incision was sutured, antibacterial/analgesic ointment applied, and the animal placed in a surgical recovery cage under a heat lamp with food and water available *ad libitum* until the effects of anesthesia had subsided, at which time they were returned to their presurgical cages.

Histology/Immunohistochemistry

At varying survival times following the last BrdU injection (days post injection, dpi), birds were deeply anesthetized with a mixture of ketamine (0.07 ml of 10 mg/ml solution; Ketaset) and xylazine (0.07 ml of a 20 mg/ml solution; Xylamed). When the birds were unresponsive to a toe-pinch they were transcardially perfused with 20 ml 0.1M PBS (pH=7.40) followed by 30 ml 4% paraformaldehyde (PFA, pH=7.40; Electron Microscopy Sciences). Brains were carefully dissected, post-fixed for 24 hrs. in 4% PFA at 4ºC, and sectioned sagittally at 50 µm on a vibratome (Leica VT1000S). We found that DARPP-32-ir was most robust and antibody binding the most specific when sections were processed within 1-2 weeks after perfusion without

cryoprotection for long term storage. Free-floating sections were permeabilized for 30 min. in 0.5% PBS-T (PBS with Triton-X 100) at room temperature on a shaker. Then, antigen retrieval was performed via 20 min. incubation in 1.5 N HCL at 37ºC in a water bath, followed by neutralization with two, 5 min. rinses in Tris base (pH=8.56; Fisher Scientific). Sections were then blocked with normal goat serum and normal donkey serum in PBS-T (3% each) for 20 min. at room temperature on the shaker. Sections were incubated overnight at 4ºC in varying mixtures of the following primary antibodies: rabbit anti-DARPP-32 (1:1000; Abcam Cat# ab40801, RRID:AB_731843), mouse anti-Hu (1:500; Molecular Probes (Invitrogen) Cat# A-21271, RRID:AB_221448), rat anti-BrdU (1:500; Bio-Rad Cat# MCA2060, RRID:AB_323427), and mouse anti-tyrosine hydroxylase (1:2000; Millipore Cat# MAB5280, RRID:AB_2201526). Following rinses in PBS-T, sections were incubated at room temperature for 90 min. in a cocktail of the following secondary antibodies: goat anti-rabbit Alexa Fluor 555 (1:500; Molecular Probes (Invitrogen) Cat# A-21429, RRID:AB_2535850), donkey anti-mouse Alexa Fluor 647 (1:500; Molecular Probes (Invitrogen) Cat# A-31571, RRID:AB_162542), and goat anti-rat Alexa Fluor 488 (1:500; Molecular Probes (Invitrogen) Cat# A-11006, RRID:AB_141373). Following 3 PBS-T rinses, sections were counterstained with Hoechst 33258 (2 ug/ml in PBS; Molecular Probes), except for tissue from the HVC_{RA} backfill experiments, which was not counterstained because FG fluoresces in the same channel as Hoechst 33258 and the overlap would have hindered interpretation. Finally, the sections were rinsed in PBS, mounted on positively charged slides (Superfrost++, Fisher Scientific), and coverslipped with Aqua-Poly/Mount (Polysciences, Inc.). Slides were then photoprotected and stored at -20ºC until confocal imaging. Negative controls were performed in which one or more primary antibodies were omitted to check for cross-reactivity.

HVC Analyses

HVC was traced using computer-yoked microscopy software (Neurolucida; MicroBrightField, Inc.), as defined by DARPP-32 staining, which was much more robust around HVC and sparser within it (Figure 2). These boundaries corresponded to the previously defined cytoarchitectural boundaries of HVC described by Fortune & Margoliash (1995) and were also identifiable with dark field microscopy. All images were analyzed in Leica Application Suite-X software (LAS-X; Leica, Inc.). Nuclear diameters were measured in LAS-X at the widest portion of the nucleus. All experimenters were blind to animal ID, hemisphere, or treatment group to ensure a lack of bias and maximum reproducibility.

Experimental Design and Statistical Analysis

For the studies of DARPP-32 expression in HVC NNs as a function of days post-BrdU injection, we included 7 groups ranging in time between final BrdU injection and sacrifice (7 – 180 dpi). The 7, 14, 21, and 90 dpi group had n=5, the 180 dpi group had n=4, the 28 dpi group had n=6, and the 45 dpi group n=7. We report the results of a one-way ANOVA for 7 samples, which along with Bonferroni post hoc tests to adjust for multiple comparisons, were performed in SPSS statistical software. We ran these one-way ANOVAs to compare 1) the *fraction* of all HVC NNs that expressed DARPP-32, calculated as DARPP-32+ HVC NNs / total HVC NNs (Figure 4B), and 2) the *density* of DARPP-32+ HVC NNs per cubic millimeter (Figure 4A). For retrograde tracing studies evaluating HVC NN connectivity, we first turned off DARPP-32 and Hu fluorescent channels in LASX and then a blinded experimenter marked all BrdU+/FG- and BrdU+/FG+ cells before turning on the other two channels to determine whether they also expressed DARPP-32, Hu, or both. For both DARPP-32+ and DARPP-32-neg HVC NNs, we calculated the fraction of the total that possessed FG, i.e. projected to RA (371 cells from 7

hemispheres from 4 birds). For nuclear diameter experiments (Figure 7), we first ran a Two factor ANOVA with repeated measures on cell type. Then, we ran paired T-tests to compare the difference between neuron types at a given dpi, and we used one way ANOVAs with Tukey's post hoc tests to analyze changes in the nuclear diameter of HVC NNs as a function of days post BrdU injection (709 cells from 20 hemispheres from 10 birds). These were performed in SPSS. For studies of DARPP-32+ neurons in HVC as a function of bird age (Figure 8), we ran a linear regression to compare the density of DARPP-32+ neurons per cubic millimeter in HVC to the age of the bird in years. These analyses were performed in Microsoft Excel.

Results

HVC NNs May Transiently Express DARPP-32

We found that approximately half of all HVC NNs express DARPP-32 at 28 dpi (50.4 ± 3.9%; Figure 3, 4A, B). To see whether DARPP-32 expression in HVC NNs changes as a function of neuronal age, we examined HVC NNs at seven time points ranging from 7 to 180 days after the last BrdU injection. We found a significant effect of neuronal age on the fraction of HVC NNs that express DARPP-32 ($F(6,30) = 101.5$, $p = 1.5 \times 10^{-18}$; Figure 4B), and on the density of DARPP-32+ HVC NNs per mm^3 ($F(6,30) = 41.1$, $p = 3.76 \times 10^{-13}$; Figure 4A). In the first month post-mitosis, we observed an increase in the fraction of HVC NNs that express DARPP-32 (Figure 4B). Tukey's post-hoc tests performed on DARPP-32+ HVC NN fractions revealed significant differences between 7 and 21 dpi ($p = 2.77 \times 10^{-11}$), 14 and 21 dpi ($p = 1.34 \times 10^{-10}$), 21 and 28 dpi ($p = 0.000006$), indicating that the number of DARPP-32+ HVC NNs in a given cohort of HVC NNs increases during the first month post mitosis. After 28 dpi we observed a decline in the fraction of DARPP-32+ HVC NNs: 28 and 45 dpi ($p = 2.22 \times 10^{-7}$), 45 and 90 dpi ($p = 2.04 \times 10^{-7}$), 45 and 180 dpi ($p = 6.39 \times 10^{-9}$), but not 90 and 180 dpi ($p = 1.00$) (Figure 4B).

Despite the decline in the density (Figure 4A) and the fraction (Figure 4B) of DARPP-32+ HVC NNs after 28 dpi, we observed no decline in the total number of HVC NNS. Taken together, these data show that there was a decrease in the fraction of DARPP-32+ HVC NNs after 28 dpi without a decline in the total density of HVC NNs over the same period (Figure 4A). This suggests that a subset of HVC NNs may transiently express DARPP-32 during their first month of development, and thereafter either turn off DARPP-32 expression or undergo apoptosis.

DARPP-32+ HVC NNs do not Project to RA

To test whether DARPP-32+ HVC NNs project to RA, we birth-dated NNs with BrdU and injected FG into RA (Figure 5A, B). Birds were killed 4 days following surgery at 32 dpi. Walton et al (2012) reported that 42% of HVC NNs project to RA at 30 dpi. Similarly, we found that 46.4% of HVC NNs examined were RA projecting (Figure 5I). When we specifically examined RA-projecting HVC NNs, we observed that they were nearly exclusively DARPP-32-negative (171/172 cells, 99.4%; Figure 5I). Moreover, all but one (125/126) DARPP-32+ HVC NNs examined were FG-, demonstrating that DARPP-32+ HVC NNs nearly exclusively do not project to RA at 32 dpi.

DARPP-32+ HVC NNs Receive Catecholaminergic Input

DARPP-32 is a reliable marker of dopaminoceptive neurons in both mammals (Hemmings, et al., 1987) and zebra finches (Rochefort, et al., 2007; Kosubeck-Langer, et al., 2017). To determine whether DARPP-32+ HVC NNs receive catecholaminergic input, we labeled tyrosine hydroxylase, the rate-limiting enzyme in the catecholamine synthetic pathway (Fernstrom & Fernstrom, 2007). At 28 dpi, all DARPP-32+ HVC NNs we examined appeared to be contacted by TH+ fibers (Figure 6; 74 cells from 3 birds). These data strongly suggest that DARPP-32+

HVC NNs receive dopaminergic input, likely from the periaqueductal gray (PAG), which is the primary source of dopaminergic afferents to HVC (Tanaka, et al., 2018).

Nuclear Diameter of DARPP-32+ HVC NNs is Transiently Larger than DARPP-32+ HVC NNs

We noticed qualitatively that DARPP-32+ HVC NNs appeared to be larger than DARPP-32-neg HVC NNs. To test this quantitatively, we measured the nuclear diameter of DARPP-32+ and DARPP-32-neg HVC NNs at 21, 28, and 45 dpi. Previous work in canaries has shown that the nuclear diameter of HVC NNs – whether RA-projecting or not – decreases between 30 and 240 dpi (Kirn, et al., 1991). In a subset of our birds (n=709 neurons from 10 birds) we evaluated whether the nuclear diameter of DARPP-32+ HVC NNS changed as a function of neuronal age, and whether it differed from DARPP-32-neg NNs (Figure 7). Two factor ANOVA with repeated measures on cell type revealed a significant main effect of neuronal age ($F(9)=22.27$, $p = 0.0009$), a significant main effect of cell type ($F(10)=240.5$, $p = <.0001$), and a significant interaction between neuronal age and cell type ($F(19) = 16$, $p = 0.0024$). We next evaluated how the nuclear diameter of each cell type changed with time. One way ANOVA revealed that the nuclear diameter of both DARPP-32-neg HVC NNs ($F(2,7)=10.8$, $p = 0.007$) and DARPP-32+ HVC NNs ($F(2,7)=27.9$, $p = 0.0005$) decreased significantly as the neurons matured (Figure 7). Tukey's post-hoc tests showed that the diameter of DARPP-32-neg HVC NNs decreased significantly between 28 and 45 dpi ($p<.01$), while the nuclear diameter of DARPP-32+ HVC NNs decreased between 21 and 45 ($p<.01$), as well as 28 and 45 dpi ($p<.01$). Finally, we showed that DARPP-32+ HVC NNs had significantly larger average nuclear diameter at 21 dpi ($t(4)=4.53$, $p=0.02$) and at 28 dpi ($t(4)=11.31$, $p=0.00009$). At 45 dpi, however, there was no difference between the average nuclear diameters of the two putative subtypes of HVC NNs ($t(4)=1.97$, $p=0.12$).

The Density of DARPP-32+ Neurons in HVC Decreases with Bird Age

In the zebra finch basal ganglia homologue Area X, NNs turn on DARPP-32 during maturation and express it indefinitely, resulting in lifelong accumulation of DARPP-32+ neurons in Area X (Kosubeck-Langer, et al., 2017). In HVC, NNs also accumulate throughout the bird's lifetime, resulting in increased neuronal packing density with increasing age (Walton, et al., 2012). However, our data suggests that DARPP-32+ expression in HVC NNs is transient (Figure 4), and we were therefore curious to see whether the density of DARPP-32+ neurons (not BrdU labeled, i.e. of indeterminate age) in HVC change as a function of increasing bird age. To test this, we quantified the density of Hu+/DARPP-32+ neurons in HVC of male zebra finches ranging from 0.5 to 7 years of age (n=23). We found a negative correlation between bird age and the density of Hu+/DARPP-32+ neurons in HVC (Figure 8; $R^2 = 0.261$, $p = 0.013$), indicating that older birds have fewer DARPP-32+ neurons in HVC than young birds.

Discussion

We report a novel subtype of HVC NN that expresses DARPP-32 during neuronal maturation and does not project to RA. We demonstrate that DARPP-32+ HVC NNs are putatively contacted by TH+ fibers and have transiently larger nuclei than DARPP-32-negative HVC NNs.

In both canaries (Alvarez-Buylla, et al., 1990) and zebra finches (Walton, et al., 2012) there is a fraction of HVC NNs that neither project to RA, nor express common markers of HVC inhibitory interneurons (Scotto-Lomassese, et al., 2007). Since it is widely accepted that Area X projecting HVC neurons are generated prenatally (Kirn, et al., 1991, 1999; Scharff, et al., 2000), this problem was commonly explained away as the young neurons not yet transporting the tracer (Kirn, et al., 1991, 1999; Scotto-Lomassese, et al., 2007). This is unlikely because at nearly 4

years post-BrdU injection, many HVC NNs still do not backfill from RA, suggesting that they never develop connections to RA or they never transport the tracer (Walton, et al., 2012). We show that one-month old DARPP-32+ HVC NNs do not backfill from RA (Figure 5). In light of these data, DARPP-32+ HVC NNs are either 1) excitatory HVC interneurons, 2) inhibitory interneurons that do not express the calcium-binding proteins that have traditionally been used to tag HVC_{INT} (parvalbumin (PV), calretinin (CR), and calbindin (CB); Wild, et al., 2005), 3) HVC_{AV} projection neurons, or 4) do not transport the tracer due to their synapse or axon type. Option 2 is unlikely because the number of GABA+ HVC_{INT} is not significantly different from the number of HVC_{INT} labeled with PV, CR, and CB combined (Wild, et al., 2005; Scotto-Lomassese, et al., 2007). Option 3 is unlikely because HVC_{AV} neurons are too sparse to account for the ~50% of non-RA-projecting HVC NNs. Roberts et al (2017) reported that HVC_{AV} neurons comprise < 1% of all HVC neurons. Just three days of BrdU injections in our birds tags many more HVC NNs (mean of 28 dpi group = 422.2 ± 86.4 NNs estimated in HVC assuming a volume of 0.25 mm^3; Walton, et al., 2012) than the estimated total number of HVC_{AV} neurons (130 ± 69.8 HVC_{AV} neurons per hemisphere; Roberts, et al., 2017). Option 4 is unlikely because Fluorogold is a highly effective retrograde tracer that rapidly (< 1 week) retrogradely labels neurons as efficiently (Yu, et al., 2015), or more efficiently (Yao, et al., 2015) than other types of retrograde tracers (e.g. Cholera toxin subunit B, Fast Blue, Fluoro-Ruby, DiI, etc). While it is possible that DARPP-32+ HVC NNs simply failed to transport the tracer due to their synapse or axon type, we believe the more likely explanation is that DARPP-32+ HVC NNs are not RA-projecting but in fact project locally as excitatory interneurons.

In Area X, a brain region necessary for song learning and maintenance, there is a steady increase in the proportion of adult-born neurons that express the immediate early gene EGR-1 (ZENK)

and DARPP-32 between 21 and 42 dpi, suggesting a link between new neuron activation, DARPP-32 expression, and successful maturation of adult-born Area X neurons (Keilani, et al., 2012; Kosubeck-Langer, et al., 2017). We found that between 7 and 28 dpi the proportion of HVC NNs expressing DARPP-32 increases to approximately 50% and then decreases despite there being no decline in the total density of HVC NNs (Figure 4A). Given that there is not a decline in HVC NNs from the same dpi time points, in conjunction with a large decline in DARPP-32+ HVC NNs, this suggests that DARPP-32+ HVC NNs are not disproportionately dying. Rather it suggests that HVC NNs are shutting off DARPP-32 expression sometime after 28 dpi.

To determine whether DARPP-32+ HVC NNs receive catecholaminergic inputs, we combined BrdU, DARPP-32, and TH immunofluorescence. At 28 dpi, all DARPP-32+ HVC NNs we examined were contacted by TH+ fibers, indicating that they receive catecholaminergic input by one month post-mitosis (74/74 cells; Figure 6). HVC receives dopaminergic inputs predominantly from the PAG and to a lesser extent, the ventral tegmental area (VTA, Appeltants, et al., 2000, 2001; Tanaka, et al., 2018). In addition to multiple types of DA receptors (Kubikova, et al., 2009), HVC contains α2-noradrenergic receptors and receives noradrenergic input from the midbrain (Riters, et al., 2002; Appeltants, et al., 2000). Hara et al (2010) showed that α2- and β1-noradrenergic receptor activation can alter the phosphorylation state of DARPP-32 at threonine-34 (thr-34) in mouse neostriatal brain slices, suggesting that DA (DA) and norepinephrine (NE) both play a role in modulating DARPP-32 phosphorylation (Hara, et al., 2010). Thr-34 is also the residue at which DARPP-32 is phosphorylated by protein kinase A following DA receptor activation (Svenningsson, et al., 2004). This raises the possibility that DARPP-32+ HVC NNs are modulated by both dopaminergic and noradrenergic inputs.

However, our TH immunofluorescence procedures did not allow us to distinguish between dopaminergic and noradrenergic terminals.

In HVC, we measured the overall number of Hu+/DARPP-32+ neurons in zebra finches aged ~0.5 to ~7 years old. We found a significant negative correlation between the density of Hu+/DARPP-32+ neurons in HVC and bird age (Figure 8). In comparing results from Fig. 8 and Fig. 4B, we believe that an argument can be made that all DARPP-32+ neurons are in fact adult-born neurons (i.e., HVC NNs). Fig. 8 shows that at about 260 dph (age range 197-321 dph), there are approximately 2500 DARPP-32+ neurons/mm3 in HVC (youngest group results in Fig. 8, n=6). Fig. 4B shows the number of DARPP-32+ neurons that are also HVC NNs, as determined by BrdU injections. If it were the case that the number of total DARPP-32+ neurons were the same as the number of DARPP-32+ neurons that were also HVC NNs, then this would suggest that all DARPP-32+ neurons are in fact HVC NNs. We don't have a direct measurement for that because we can only label HVC NNs from discrete time points using BrdU; that is, only those neurons that are dividing during the BrdU injections are labeled, and it's implausible to inject BrdU every day. However, we can sum the columns in Fig. 4B to produce a conservative estimate of how many HVC NNs are at some point DARPP-32+. Adding up all the columns (i.e., 7, 14, and 21 dpi) leading up to the 28 dpi peak represents about 800 neuron/mm3. Given that these intervals (7, 14, 21 dpi) are only capturing a minimum of half of all the newborn neurons during that time period (i.e., BrdU injections over 3 days—not each of the 7 day intervals between), then it's reasonable to double those numbers, i.e., 800 * 2 = 1600 neurons/mm3. Summing 1600 to the 800 neurons/mm^3 measured at the 28 dpi peak yields an estimate of 2400 DARPP-32+ NNs/mm^3 at 220 dph (age range 197-321 dph at time of BrdU injection). This

conservative estimate is close to the 2500 NNs/mm^3 of all DARPP-32+ shown in Figure 8, thus suggesting that nearly all DARPP-32+ neurons are in fact HVC NNs.

Considering this estimate and the decline in DARPP-32+ neurons with age that is similar to the decline in HVC neurogenesis with age (Wang et al., 2002), and in addition to RA-projection results in Figure 5I and timeline for DARPP-32+ expression in Figure 4, leads us to propose the following hypothesis: in zebra finch HVC, DARPP-32 expression is a marker of HVC NNs that are probably less than 180 days old and are not RA projection neurons. Given the relative ease of DARPP-32+ staining, this could be a great aid in further studies investigating neurogenesis in vocal learning. It should, however, be noted that lack of DARPP-32 expression is not conclusive with regards to HVC NN status, as DARPP-32+ expression is transitory.

Herein we further characterize a class of previously identified HVC NNs about which very little has been reported. We show that these neurons express DARPP-32, receive putative catecholaminergic synaptic contacts, and do not retrogradely trace from RA as part of the vocal motor pathway.

References

Alvarez-Buylla A, Kirn JR, Nottebohm F (1990) Birth of projection neurons in adult avian brain may be related to perceptual or motor learning. Science 249(4975):1444-1446.

Appeltants D, Absil P, Balthazart J, Ball GF (2000) Identification of the origin of catecholaminergic inputs to HVc in canaries by retrograde tract tracing combined with tyrosine hydroxylase immunocytochemistry. J Chem Neuroanat 18:117-133

Appeltants D, Ball GF, Balthazart J (2001) The distribution of tyrosine hydroxylase in the canary brain: demonstration of a specific and sexually dimorphic catecholaminergic innervation of the telencephalic song control nuclei. Cell Tissue Res 304:237-259.

Barker JM, Charlier TD, Ball GF, Balthazart J (2013) A new method for in vitro detection of bromodeoxyuridine in serum: a proof of concept in a songbird species, the canary. PLoS ONE 8(5): e63692. doi:10.1371/journal.pone.0063692

Burek MJ, Nordeen KW, Nordeen EJ (1994) Ontogeny of sex differences among newly generated neurons of the juvenile avian brain. Devel Brain Res 78:57-64.

DeWulf V, Bottjer SW (2005) Neurogenesis within the juvenile zebra finch telencephalic ventricular zone: a map of proliferative activity. J Comp Neurol 481:70-83.

Fernstrom JD, Fernstrom MH (2007) Tyrosine, phenylalanine, and catecholamine synthesis and function in the brain. J Nutr 137:1539S–1547S.

Fortune ES, Margoliash D (1995) Parallel pathways and convergence onto HVc and adjacent neostriatum of adult zebra finches (Taeniopygia guttata). J Comp Neurol 360:413-441.

Hara M, Fukui R, Hieda E, Kuroiwa M, Bateup HS, Kano T, Greengard P, Nishi A (2010) Role of adrenoreceptors in the regulation of DA/DARPP-32 signaling in neostriatal neurons. J Neurochem 113(4):1046-1059.

Hemmings Jr HC, Walaas SI, Ouimet CC, Greengard P (1987) Dopaminergic regulation of protein phosphorylation in the striatum: DARPP-32. Trends Neurosci 10:377–383.

Jarvis ED, Scharff C, Grossman MR, Ramos JA, Nottebohm F (1998) For whom the bird sings: context dependent gene expression. Neuron 21:775-788

Keilani S, Chandwani S, Dolios G, Bogush A, Beck H, Hatzopoulos AK, Rao GN, Thomas EA, Wang R, Ehrlich ME (2012) Egr-1 induces DARPP-32 expression in striatal medium spiny neurons via a conserved intragenic element. 32(20):6808-6818.

Kirn JR, & DeVoogd TJ (1989) Genesis and death of vocal control neurons during sexual differentiation in the zebra finch. J Neurosci 9(9):3176-3187.

Kirn JR, Alvarez-Buylla A, Nottebohm F (1991) Production and survival of projection neurons in the forebrain center of adult male canaries. J Neurosci 11(6):1756-1762.

Kirn JR, Fishman Y, Sasportas K, Alvarez-Buylla A, Nottebohm F (1999) Fate of new neurons in adult canary high vocal center during the first 30 days after their formation. J Comp Neurol 411:487-494.

Kosubeck-Langer J, Schulze L, Scharff C (2017) Maturation, behavioral activation, and connectivity of adult-born medium spiny neurons in a striatal song nucleus. Front Neurosci 11:323. doi: 10.3389/fnins.2017.00323

Kubikova L, Wada K, Jarvis ED (2009) DA receptors in a songbird brain. J Comp Neurol 518:741-769.

Nixdorf-Bergweiler BE, Bischof HJ (2007) A stereotaxic atlas of the brain of the zebra finch, Taeniopygia guttata: with special emphasis on telencephalic visual and song system nuclei in transverse and sagittal sections. Bethesda, MD: NCBI.

Ouimet CC, Greengard P (1990) Distribution of DARPP-32 in the basal ganglia: an electron microscopic study. J Neurocytol 19:39-52.

Pytte CL (2016) Adult neurogenesis in the songbird: region-specific contributions of new neurons to behavioral plasticity and stability. Brain Behav Evol 77:191-204.

Roberts TF, Hisey E, Tanaka M, Kearney M, Chattree G, Yang C, Shah NM, Mooney R (2017) Identification of a motor to auditory pathway important for vocal learning. Nat Neurosci 20(7):978-986.

Rochefort C, He X, Scotto-Lomassese S, Scharff C (2007) Recruitment of FoxP2-expressing neurons to Area X varies during song development. Dev Neurobiol 67(6):809-817

Riters L, Eens M, Pinxten R, Ball GF (2002) Seasonal changes in the densities of a2-noradrenergic receptors are inversely related to changes in testosterone and the volumes of song control nuclei in male European starlings. J Comp Neurol 444-63-74.

Scharff C, Kirn JR, Grossman M, Macklis JD, Nottebohm F (2000) Targeted neuronal death affects neuronal replacement and vocal behavior in adult songbirds. Neuron 25:481-492.

Scott BB, Lois C (2007) Developmental origin and identity of song system neurons born during vocal learning in songbirds. J Comp Neurol 502:202-214.

Scotto-Lomassese S, Rochefort C, Nshdejan A, Scarff C (2007) HVC interneurons are not renewed in adult male zebra finches. Eur J Neurosci 25(6):1663-1668.

Shaughnessy DW, Hyson RL, Bertram R, Wu W, Johnson F (2019) Female zebra finches do not sing yet share neural pathways necessary for singing in males. J Comp Neurol 527(4):843-855.

Shevchouk OT, Ball GF, Cornil CA, Balthazart J (2017) Studies of HVC plasticity in adult canaries reveal social effects of sex differences as well as limitation of multiple markers available to assess adult neurogenesis. PLoS One 12(1): e0170938. doi:10.1371/journal.pone.0170938

Singh UA & Iyengar S (2019). The expression of DARPP-32 in adult male zebra finches (Taenopygia guttata). Brain Struct Funct 224(8):2939-2972.

Sohrabji F, Nordeen EJ, Nordeen KW (1993) Characterization of neurons born and incorporated into a vocal control nucleus during avian song learning. Brain Res 620:335-338.

Svenningsson P, Nishi A, Fisone G, Girault JA, Nairn A, & Greengard P (2004). DARPP-32: an integrator of neurotransmission. Annu. Rev. Pharmacol. Toxicol. 44:269-296.

Tanaka M, Sun F, Li Y, Mooney R (2018) A mesocortical DA circuit enables the cultural transmission of vocal behavior. Nature 563(7729):117-120.

Tokarev K, Boender AJ, Claβen GAE, Scharff C (2016) Young, active and well-connected: adult-born neurons in the zebra finch are activated during singing. Brain Struct Funct 221:1833-1843.

Walaas SI, Greengard P (1984) DARPP-32, a DA- and adenosine 3’:5’-monophosphate-regulated phosphoprotein enriched in DA-innervated brain regions. Regional and cellular distribution in the rat brain. J Neurosci 4(1):84-98.

Walton C, Pariser E, Nottebohm F (2012) The zebra finch paradox: song is little changed, but number of new neurons doubles. J Neurosci 32(3):761-774.

Wang N, Hurley P, Pytte C, Kirn JR (2002) Vocal control neuron incorporation decreases with age in the adult zebra finch. J Neurosci 22(24):10864-10870.

Wild JM, Williams MN, Howie GJ, Mooney R (2005) Calcium-binding proteins define interneurons in HVC of the zebra finch (Taeniopygia guttata). J Comp Neurol 483:76-90.

Wood WE, Roseberry TK, & Perkel DJ (2013). HTR2 receptors in a songbird premotor cortical-like area modulate spectral characteristics of zebra finch song. J Neurosci 33(7):2908-2915.

Yao F, Zhang E, Gao Z, Ji H, Marmouri M, Xia X (2018) Did you choose appropriate tracer for retrograde tracing of retinal ganglion cells? The differences between cholera toxin subunit B and Fluorogold. PLoS ONE 13(10): e0205133. https://doi.org/10.1371/journal.pone.0205133

Yu Yl, Li Hy, Zhang Px, Yin Xf, Han N, Kou Yh, Jiang Bg. Comparison of commonly used retrograde tracers in rat spinal motor neurons. Neural Regen Res 2015;10:1700-5

Figures

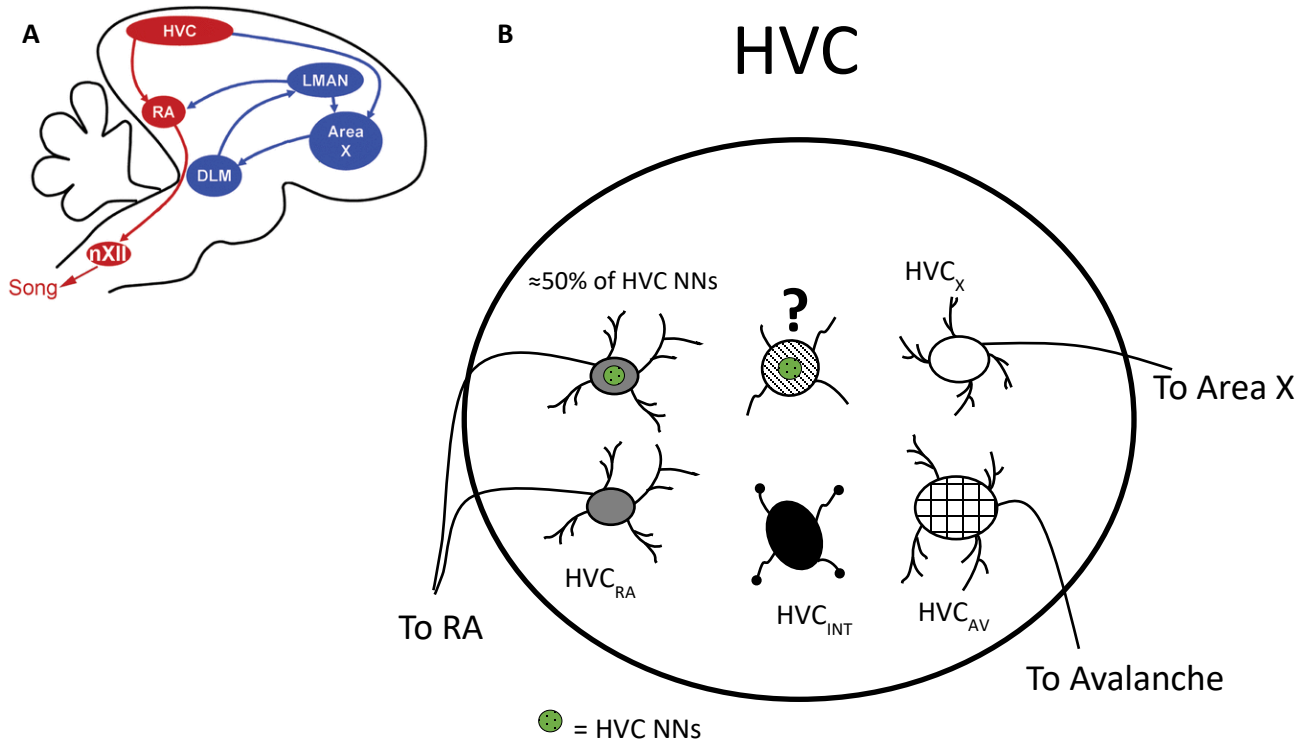

Figure 1. Organization of HVC and the zebra finch song system. (A) Schematic of a sagittal view of the zebra finch brain showing the song system brain regions that comprise the vocal motor pathway (red) and the anterior forebrain pathway (blue). Posterior is to the left, ventral is down. Reproduced with permission from Wood et al 2013. (B) Schematic of HVC showing known populations of HVC neurons. Green stippled circles are BrdU+ nuclei meant to distinguish those generated postnatally from those of generated prenatally. The question mark represents the approximately 50% of HVC NNs that do not project to RA and which have not been well characterized.

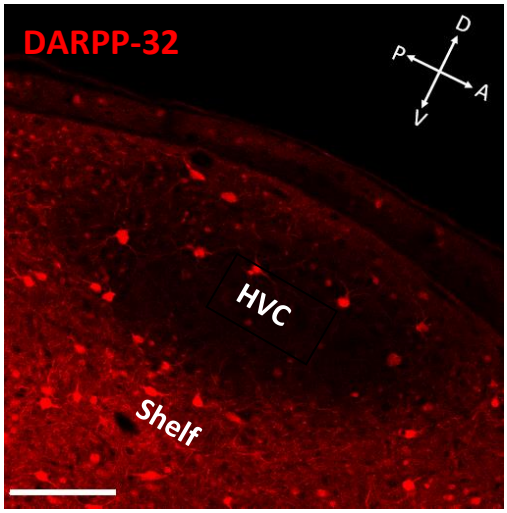

Figure 2. Confocal photomicrograph of HVC in sagittal section showing DARPP-32 labeling using a monoclonal antibody (ab40801) that recognizes and binds to DARPP-32 independent of its current phosphorylation state. There are fewer labeled cells in HVC compared to the underlying HVC shelf region, which, like much of the surrounding nidopallium, labels much more robustly for DARPP-32 than within HVC (Singh & Iyengar, 2019). 23.8X, scale bar = 100 µm.

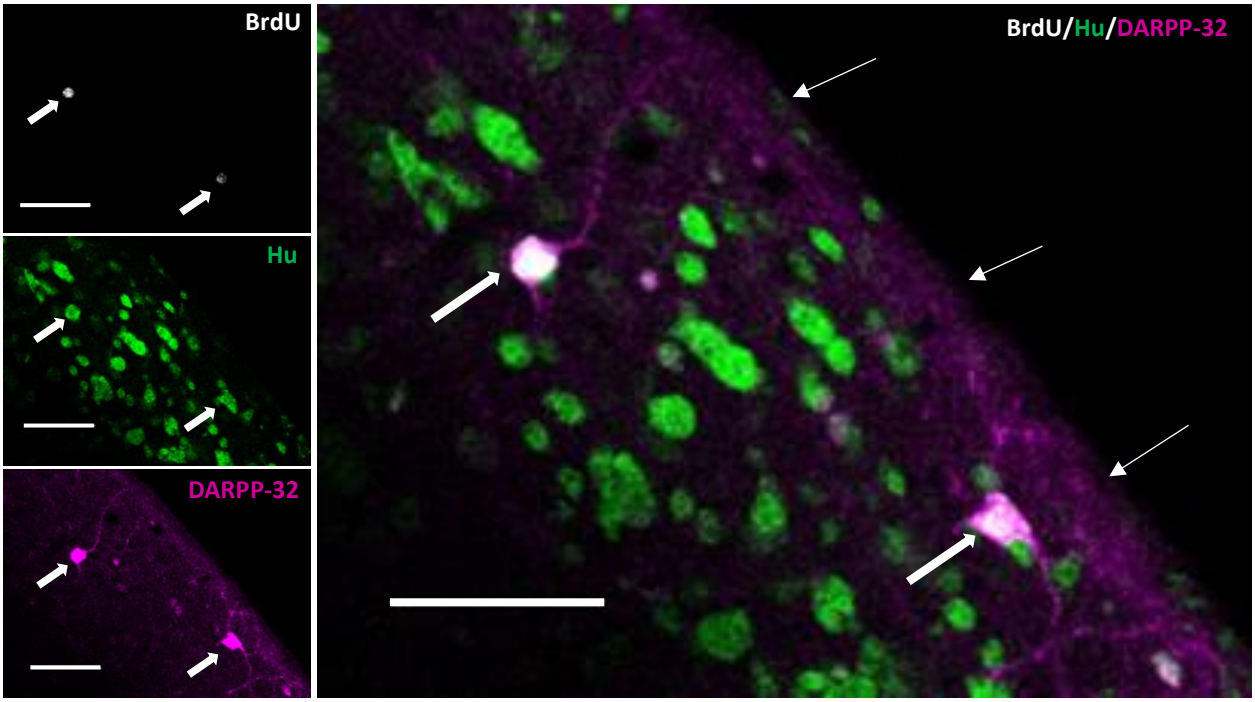

Figure 3. 28-day old HVC NNs express the phosphoprotein DARPP-32. Confocal photomicrograph of a single plane of section of the same field of view in dorsal HVC showing two DARPP-32+ NNs at 28 dpi. (A) BrdU labeled nuclei, (B) Neurons labeled for the neuron-specific protein Hu, (C) DARPP-32+ neurons, (D) merged image of all three channels; thick arrows indicate triple-labeled BrdU+/Hu+/DARPP-32+ HVC NNs at 28 dpi. Thin arrows indicate the dorsal surface of HVC. 18x magnification. Scale bars = 25 µm.

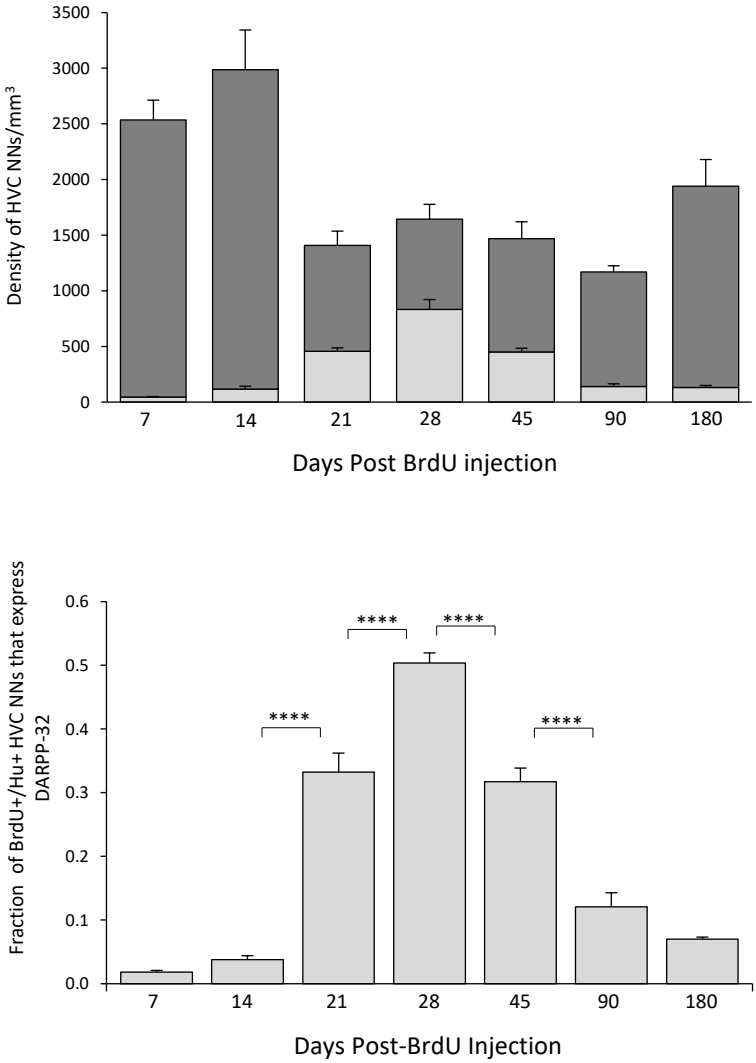

Figure 4. DARPP-32 expression in HVC NNs changes as a function of neuronal age. (A) The density of HVC NNs as a function of days following the final BrdU injection. Light gray bars represent BrdU+/Hu+/DARPP-32+ HVC NNs, dark gray bars represent BrdU+/Hu+/DARPP-32-negative HVC NNs. The total height of the stacked bars equals the average density of HVC NNs per cubic millimeter. From 21 dpi on we observed no statistically significant decline in the density of HVC NNs. Over the same period there is a substantial decline in the density of DARPP-32+ HVC NNs. Group sizes are as follows: 7, 14, 21, and 90 dpi, n=5; 28 dpi, n=6; 45 dpi, n=7; 180 dpi, n = 4. (B) To determine the fraction of HVC NNs that express DARPP-32 at

each time point sampled, we divided the density of DARPP-32+ HVC NNs (BrdU+/Hu+/DARPP-32+) by the density of all HVC NNs (BrdU+/Hu+); these values are presented here as a derivation of the data in 4A. These data show that the fraction of HVC NNs that express DARPP-32 increases to approximately 50% at 28 dpi and thereafter declines. Error bars represent SEMs.

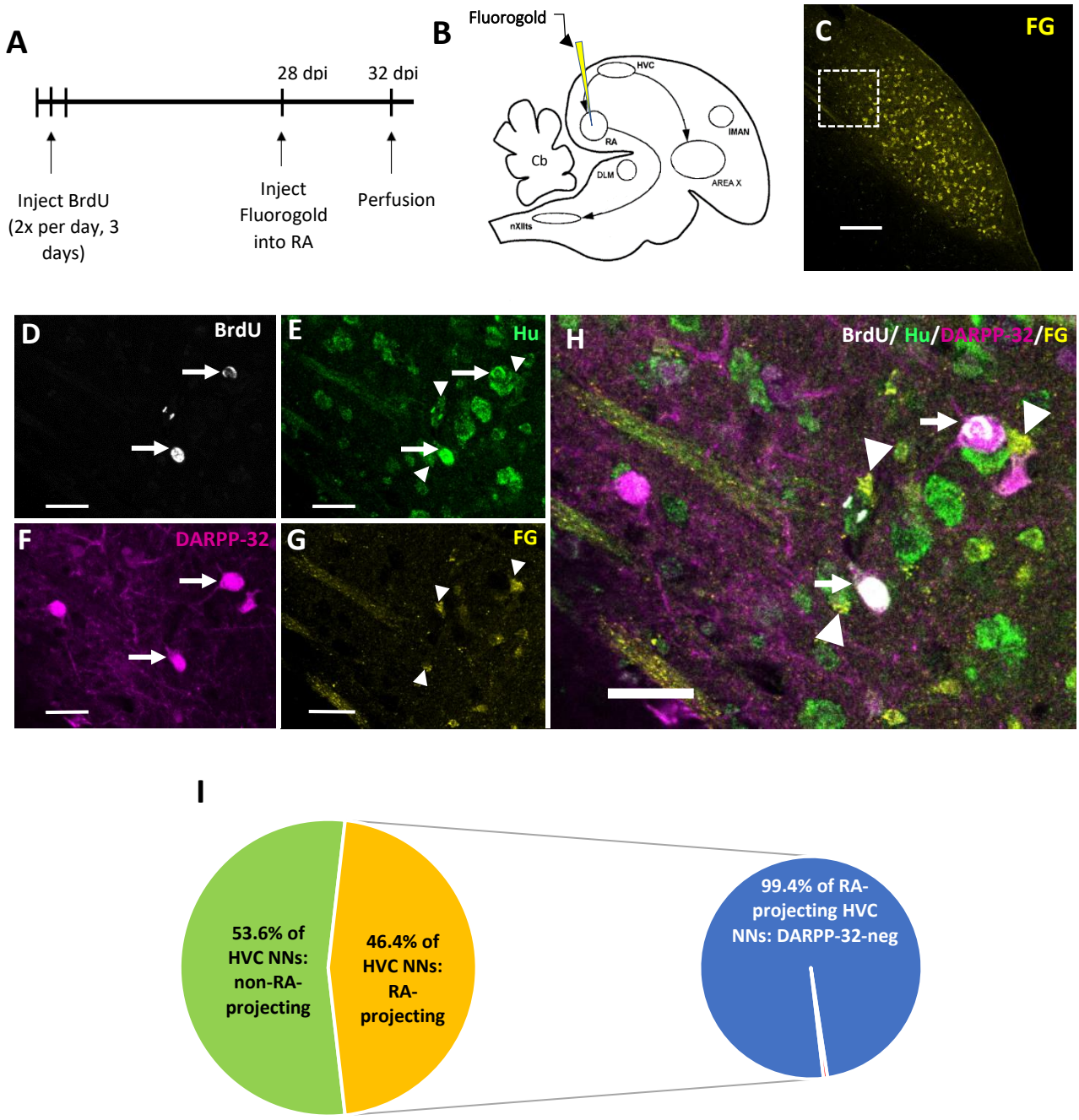

Figure 5. DARPP-32+ HVC NNs do not project to RA at 32 dpi. **(A)** Timeline of HVC_{RA} backfill experiments. **(B)** Simplified schematic of the song system in sagittal section showing some of the brain regions involved in song production. The retrograde tracer Fluorogold (FG)

was injected into RA to backfill HVC_{RA} neurons. **(C)** Maximum intensity projection of Z-stack showing backfilled FG+, RA-projecting neurons in HVC (18x; scale bar = 100 µm). Dotted white box delineates the area in HVC examined at higher magnification in panels D-H (18x, scale bar = 100 µm). **(D-H)** Confocal photomicrograph showing DARPP-32+ HVC NNs (white arrows) in HVC that did not backfill from RA. **(D)** BrdU+ nuclei. **(E)** Hu+ neurons. **(F)** DARPP-32+ neurons. **(G)** FG+ neurons. **(H)** Merged image of all four channels showing DARPP-32+ HVC NNs that do not backfill from RA (white arrows), surrounded by Hu+/FG+/DARPP-32-negative HVCRA neurons (white arrowheads). 50x, scale bar = 25 µm. **(I)** 125/126 DARPP-32+ HVC NNs we examined were FG-negative. 32-34 day old DARPP-32+ HVC NNs do not backfill from RA. 53.6% of HVC NNs examined (green; 199/371) did not project to RA, while 46.4% did project to RA (yellow; 172/371 neurons), as measured by whether or not the somata were FG+. Of the 46.4% of RA-projecting HVC NNs, only 1/172 was DARPP-32+, suggesting that DARPP-32+ HVC NNs do not project to RA at 32 dpi.

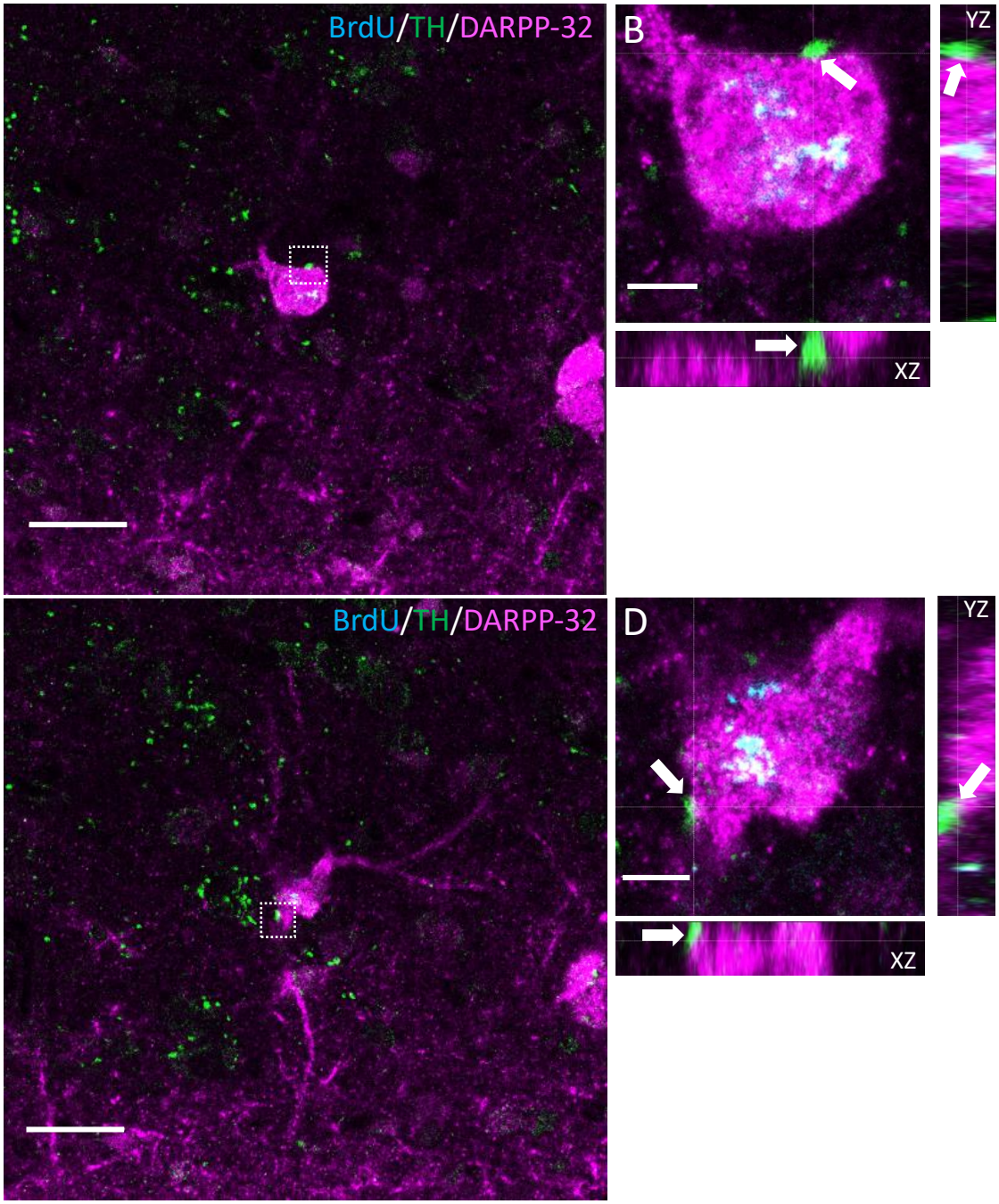

Figure 6. DARPP-32+ HVC NNs are contacted by tyrosine hydroxylase fibers. **(A,C)** Confocal photomicrographs of the same DARPP-32+ HVC NN at two different levels in the Z-stack, showing two different putative TH synaptic contacts. **(B,D)** High magnification orthogonal

views of the synaptic contacts shown in the dotted white boxes in images **A** and **C**. Scale bars: 10 um: **(B, D)**, 25 um **(A, C)**. Magnification: 75.2x **(A,C)**, 140x (**B,D)**.

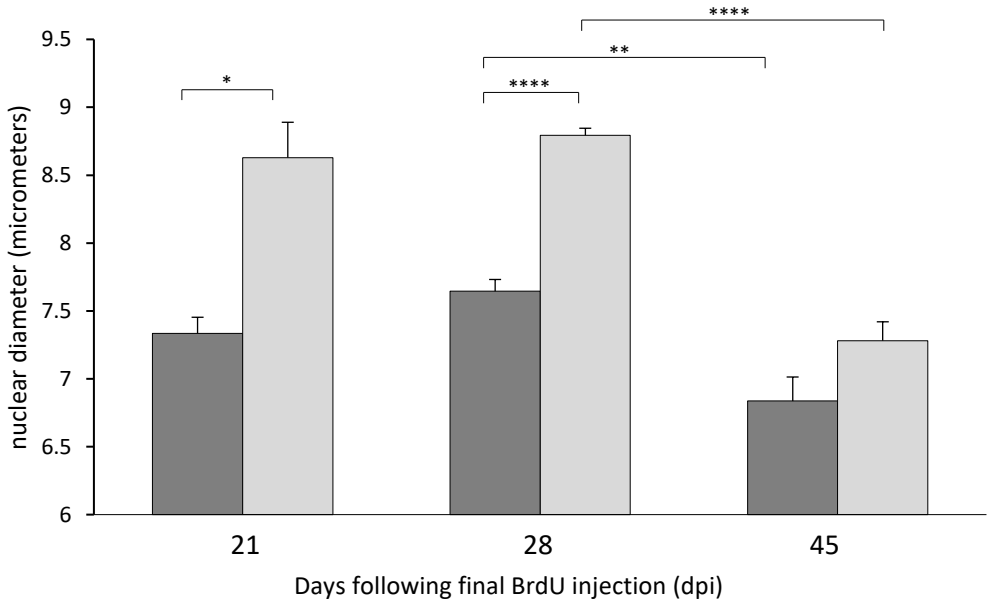

Figure 7. Mean nuclear diameter of HVC NNs over the 45 days post-BrdU injection. The nuclear diameter of DARPP-32+ HVC NNs (light gray bars) was significantly larger than that of DARPP-32-neg HVC NNs (dark gray bars) at 21 dpi, and at 28 dpi. However, at 45 dpi, there was no significant difference between the mean nuclear size of the two subtypes of HVC NNs. Statistics revealed that both subtypes of new neurons demonstrated a decline in nuclear diameter with increasing neuronal age.

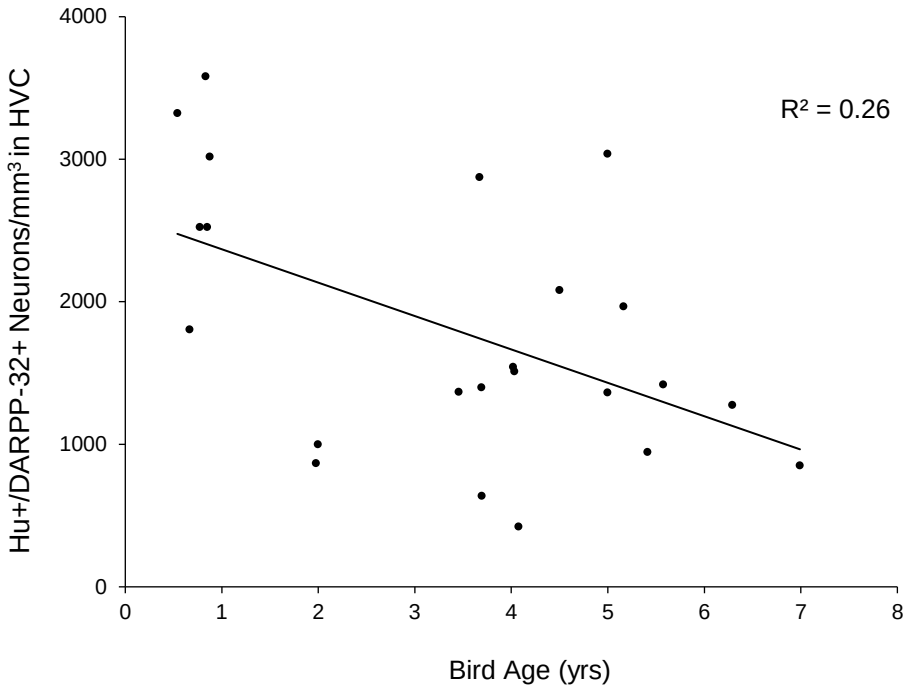

Figure 8. The density of Hu+/DARPP-32+ neurons in HVC decreases with bird age. **(A)** Older birds had fewer DARPP-32+ neurons in HVC ($r = -0.51$, $p = 0.013$, $R^2 = 0.26$). Each dot represents one bird. These neurons were not birth-dated; old birds did not receive BrdU injections, and therefore these neurons are of indeterminate age.